Morten Foldager Pedersen, Karen Filbee-Dexter, Kjell Magnus Norderhaug, Stein Fredriksen, Nicolai Lond Frisk, Camilla With Fagerli & Thomas Wernberg. 2020. Detrital carbon production and export in high latitude kelp forests. Oecologia. 192: 227–239

Detrital carbon production and export in high latitude kelp forests

Morten Foldager Pedersen*[1)], Karen Filbee-Dexter[2,3)], Kjell Magnus Norderhaug[3)], Stein Fredriksen[4)], Nicolai Lond Frisk[1)], Camilla With Fagerli[2)] and Thomas Wernberg[1,5)]

[1)] Department of Science and Environment (DSE), Roskilde University, DK-4000 Roskilde, Denmark.

[2)] Norwegian Institute of Water Research (NIVA), N-0349 Oslo, Norway.

[3)] Institute of Marine Research (IMR), 4817 His, Norway.

[4)] Department of Bioscience, University of Oslo, N-0316 Oslo, Norway.

[5)] UWA, Oceans Institute and School of Biological Sciences, University of Western Australia, 6009 Crawley, WA, Australia.

*corresponding author: email: mfp@ruc.dk

Running page head: Detrital production in *Laminaria hyperborea*.

ABSTRACT

The production and fate of seaweed detritus is a major unknown in the global C-budget. Knowing the quantity of detritus produced, the form it takes (size) and its timing of delivery are key to understanding its role as a resource subsidy to secondary production and/or its potential contribution to C-sequestration. We quantified the production and release of detritus from 10 *Laminaria hyperborea* sites in northern Norway (69.6ºN). Kelp biomass averaged 770 ± 100 g C m^{-2} while net production reached 499 ± 50 g C m^{-2} y^{-1}, with most taking place in spring when new blades were formed. Production of biomass was balanced by a similar formation of detritus (478 ± 41 g C m^{-2} y^{-1}), and both were unrelated to wave exposure when compared across sites. Distal blade erosion accounted for 23% of the total detritus production and was highest during autumn and winter, while dislodgment of whole individuals and/or whole blades corresponded to 24% of the detritus production. Detachment of old blades constituted the largest source of kelp detritus, accounting for >50% of the total detrital production. Almost 80% of the detritus from *L. hyperborea* was thus in the form of whole plants or blades and > 60% of that was delivered as a large pulse within 1-2 months in spring. The discrete nature of the delivery suggests that the detritus cannot be retained and consumed locally, and that some is exported to adjacent deep areas where it may subsidize secondary production or become buried into deep marine sediments as blue carbon.

Key words: detritus, seaweed, drift, resource subsidy, carbon sequestration

INTRODUCTION

Flow of dead organic matter (detritus) across ecosystem boundaries connects neighboring ecosystems and may fuel secondary productivity in recipient ecosystems where primary productivity is low. Detrital subsidies can alter patterns of species composition and food web structure in terrestrial and aquatic systems (e.g. Polis et al. 1997), but may be particularly important in aquatic environments due to greater connectivity than in terrestrial systems (Carr et al. 2003). The productivity of kelp-dominated ecosystems may exceed 2000 g C m^{-2} y^{-1} (Mann 1973, Abdullah & Fredriksen 2004) although rates in the range of 4 - 600 g C m^{-2} y^{-1} are more common (e.g. Krumhansl & Scheibling 2012, Pessarrodona et al. 2018, Wernberg et al. 2019). Direct grazing on live kelp is often low and ranges from 10 to 15% of the annual production (Krumhansl & Scheibling 2012), although grazing by sea urchins and herbivorous fishes can be high in disturbed systems (Poore et al. 2012, Wernberg et al. 2013, Steneck & Johnson 2013). Most kelp production is therefore channeled to the detrital pool within kelp systems or in adjacent systems such as beaches (Columbini & Chelazzi 2003, Ince et al. 2007), seagrass beds (Wernberg et al. 2006), distant reefs (Vanderklift & Wernberg 2008), deeper sub-tidal areas (Filbee-Dexter & Scheibling 2016) and submarine canyons (Vetter & Dayton 1999), where it may be consumed by detritivores, decompose or accumulate and, thus, contribute to C-sequestering (Cebrian 1999, Krause-Jensen & Duarte 2016).

Kelp detritus is generated through different processes such as continuous erosion and/or pruning of the blades and dislodgement of entire plants or whole blades, including phenologically determined losses of old blades in some species (Krumhansl & Scheibling 2012). Most studies to date have either quantified detritus formation through dislodgement or through blade erosion (table 1 in Krumhansl & Scheibling 2012), while only three studies have conducted concurrent measurements of erosion and dislodgment rates that allow

68 comparisons of the relative contribution of detritus formed by these different processes
69 (Gerard 1976, de Bettignies et al. 2013b, Pessarrodona et al. 2018).
70 The relative importance of the mechanisms of detritus formation may be context
71 dependent and vary as a function of species and environmental conditions. Dislodgement
72 caused by strong water movement is often considered the main driver for production of kelp
73 detritus, due to higher kelp mortality during periods of peak wave action (e.g. Ebeling et al.
74 1985, Seymour et al. 1989, Graham et al. 1997) and because large amounts of kelp detritus
75 accumulate as beach cast or in adjacent deep habitats following storms (e.g. Griffiths et al.
76 1983, Filbee-Dexter & Scheibling 2012). Other studies have shown that the formation of
77 detritus through distal erosion of blades can be significant and match annual blade production
78 (e.g. Krumhansl & Scheibling 2011a, de Bettignies et al. 2013b). Blade erosion may be
79 positively correlated to water movement, but may also be stimulated by epiphytic load (e.g.
80 bryozoans), grazing and seasonal patterns of reproduction that may weaken the blade tissue
81 and make it more susceptible to scouring (Krumhansl & Scheibling 2011b, de Bettignies et al.
82 2012, 2013b, Mohring et al. 2012). Detritus generated by these different processes varies
83 substantially in size (from small particles to whole thalli), which may affect dispersal range,
84 consumption and decomposition rate.
85 *Laminaria hyperborea* (Gunnerus) Foslie is the dominant kelp species in terms of
86 biomass along rocky shores in the NE Atlantic where it forms extensive forests that dominate
87 coastal primary production (e.g. Smale et al. 2013, Pessarrodona et al. 2018, Wernberg et al.
88 2019). *L. hyperborea* produces one annual blade that begins to form in winter and grows to
89 maximum size (~1 m^2) during spring and early summer, after which it erodes during fall and
90 winter. The remains of the blade are shed in spring as the new, emerging blade is formed at
91 the base of the old. A large proportion of the old blade biomass is thus discharged over a short
92 period, which may result in a significant pulse of coarse detritus (Pessarrodona et al. 2018).

93 The overall aim of this study was to quantify the spatial and seasonal variation in productivity
94 and formation of detritus through erosion, dislodgement, and the spring cast of old blades for
95 high latitude populations of *Laminaria hyperborea*. We expected that physical forcing caused
96 by waves would be an important driver for spatial and temporal variations in the formation of
97 kelp detritus through erosion and dislodgment, while the spring cast of old blades would
98 constitute a substantial pulse of coarse kelp detritus.
99
100 **METHODS**
101 **Study site.** Our study took place around the mouth of Malangen fjord in northern Norway
102 (69.6° N, 18.0° E). The area is heavily influenced by ocean swells, wind generated waves and
103 tides (±1.5 m). The rocky subtidal is dominated by kelp *Laminaria hyperborea* to a depth of
104 ca. 20-25 m. The study area covers 126 km^2 of coastal ocean (Fig. 1) of which *L. hyperborea*
105 covers ca. 22 km^2 according to a predictive kelp forest model developed by the national
106 Norwegian mapping of marine habitats (Bekkby et al. 2013). The model uses 12 years of
107 monitoring data for the entire Norwegian coast along with wind, fetch, coastline and
108 bathymetric data to predict the presence/absence of kelp. We selected ten study sites
109 representing a range of wave exposure levels based on variations in effective fetch (Fig. 1),
110 with the most exposed site on a shoal 2.4 km offshore (site 5), and the most protected site in a
111 small bight 3.5 km in from the mouth of the fjord (site 10). The sites ranged from 'moderately
112 exposed' to 'very exposed' according to the EUNIS classification system used to classify
113 coastal habitats in Europe (Davies & Moss 2003). We quantified kelp density, biomass,
114 production, and formation of detritus through different processes at each site during autumn
115 2016, winter 2016-2017, spring 2017 and summer 2017.
116
117 **Temperature, light and wave exposure.** Water temperature and light intensity in the kelp

forests (just above the canopy) were monitored hourly at each sampling site during the entire study period using HOBO data loggers (Pendant Temp-Light, Onset Computer Corporation) anchored to subsurface floats. Wave exposure level was calculated for each site from August 2016 to August 2017 using a modified version of the method presented by Fonseca & Bell (1998). Hourly wind data (mean velocity and direction) were obtained from Hekkingen Lighthouse weather station (the Norwegian Metrological Institute) located in the middle of the study area. Weighted effective fetch (*WEF*) for each sampling site was estimated by placing the center of a circle on all sites and subsequently dividing each of these into 8 sectors each with an angle of 45°, beginning at the N sector (337.5° - 22.5°). The fetch (*F* in km) was measured along 5 radia (each with 11.25° spacing) within each sector and the weighted effective fetch for each sector (WEF_i) was then estimated by first multiplying each fetch with the cosine of the angle (γ) of departure from the major heading (of the sector) and finally averaging the 5 values:

$$WEF_i = (\Sigma\ (F_i \times \cos\ \gamma_i)) / 5 \qquad \text{(Eq. 1)}$$

Relative wave exposure index (*REI*) was computed hour by hour for each site by multiplying hourly wind speeds with the relevant effective fetch:

$$REI = WEF_i \times V_i \qquad \text{(Eq. 2)}$$

where i is the i^{th} compass heading (i.e. 1 to 8 [N, NE, E, etc.] in 45º increments) and V_i is the wind speed from direction i. Hourly estimates of *REI* were finally used to estimate mean and maximum *REI* for each site during autumn (18^{th} Aug – 25^{th} Oct), winter (26^{th} Oct – 29^{th} March), spring (2^{nd} April – 29^{th} May) and summer (30^{th} May – 10^{th} Aug), respectively. Maximum *REI* was estimated as the average of the 10% highest *REI*-values in a season.

Kelp density and biomass. The density and biomass of kelp were quantified in August and October 2016 and in March, May and August 2017. SCUBA divers collected all canopy

143 plants (i.e. plants with stipes longer than ca. 0.7 m, Pedersen et al. 2012) within 4 to 6
144 quadrats (area = 0.25 m^2) at each site. The quadrats were placed haphazardly in the kelp forest
145 at 5 - 7 m depth and with a minimum distance of 5 m apart. Density was quantified by
146 counting the number of canopy plants in each quadrat. The fresh weight (FW) biomass of
147 each individual stipe and blade (both old and new blades in March and May) was weighed to
148 the nearest gram and total FW biomass per quadrat was estimated as the sum of all individual
149 weights of canopy plants. Holdfasts were not collected, but they comprise ca. 13% (±4) of the
150 FW biomass of the whole thallus (Pedersen et al. 2012, Bekkby et al. 2014).
151
152 **Blade growth and erosion.** Modified versions of the hole punch methods were used to
153 measure frond elongation (Parke 1948) and distal erosion of the blade (Tala & Edding 2005).
154 Twenty kelp individuals were tagged for growth and erosion measurements at each site and
155 field campaign and harvested during the succeeding campaign. The kelps were tagged with
156 two holes in the lower, basal part of the blade for growth measurements (5 and 10 cm above
157 the junction between the stipe and the blade, i.e. the meristem) and three holes in the distal
158 part of the blade (10, 20 and 30 cm from the distal edge of the blade) for erosion
159 measurements. Tagged individuals were marked with yellow cable ties around the top of the
160 stipe to ease identification and harvest during the following field campaign. Blade elongation
161 was quantified by measuring the distance from the lowest hole to the meristem (*bd1*) and the
162 distance between the two basal holes (*bd2*). Blade elongation (*BE*) was calculated by
163 subtraction of the sum of these two measures by 10 cm:
164 $$BE = (bd1 + bd2) - 10 \quad \text{Eq. 3}$$
165 The distance from the distal edge of the blade to each of the three terminal holes (*td1*, *td2* and
166 *td3*, respectively) was also measured and blade erosion (*ER*) was calculated by subtracting 10,

20 and 30 cm, respectively, from the measured distances from the edge to each of the three terminal holes and averaging the results:

$$ER = ((td1 - 10) + (td2 - 20) + (td3 - 30)) / 3 \quad \text{Eq. 4}$$

Each blade was finally cut in 5 cm segments that were weighed (blotted FW). The heaviest segment from the basal half of the blade was used to calculate daily blade production per individual (BP, g FW individual^{-1} d^{-1}) using Eq. 5:

$$BP = BE \times FW_B \times t^{-1} \quad \text{Eq. 5}$$

where BE is blade elongation (in cm), FW_B is the length specific biomass (g FW cm^{-1}) of the heaviest segment from the basal half of the blade, and t is the number of days elapsed between tagging the plant and its harvest. The heaviest segment from the lower half of the lamina was used to calculate production because the density (g FW unit^{-1} area) continues to increase after the elongation rate has ceased. Blade production (g DW m^{-2}) was finally estimated by multiplying daily blade production per individual (BP) with plant density and the number of days elapsed between sampling events. Stipe production was not measured in the present study but was estimated from measured stipe biomass from the above quadrat collections and P/B-ratios for canopy plant stipe (P/B-ratio = 0.234 ± 0.032 [mean ± sd]); Pedersen et al. 2012).

Segments from the distal half of the blade were used to calculate the biomass of eroded blade material (B_E) by multiplying the erosion length (ER) with the average length specific biomass (FW_D cm^{-1}) of the distal half of the blade according to Eq. 6:

$$B_E = ER \times FW_D \times t^{-1} \quad \text{Eq. 6}$$

where t is the number of days elapsed between tagging the plants and its collection. Blade erosion losses (g DW m^{-2}) was finally estimated by multiplying daily blade erosion per individual (B_E) with plant density and the number of days elapsed between sampling events.

192 **Dislodgement and spring cast.** Dislodgement of whole plants and blades was estimated as
193 the proportion of tagged plants that was lost between sampling events and from the number of
194 'fresh' stipes without blades (i.e. with destroyed meristems) collected in the quadrats. The
195 mass of kelp detritus formed by dislodged plants (D_{DIS}) was estimated as the site-specific
196 proportion of plants lost between sampling events (P_L) multiplied by site-specific kelp density
197 (D) and individual kelp biomass (B_{IND}) to obtain daily losses in g FW m^{-2} between sampling
198 events:

199 $$D_{DIS} = P_L \times D \times B_{IND} \times t^{-1} \quad \text{Eq. 7}$$

200 where t is the time elapsed between two succeeding sampling events. The biomass of old
201 lamina lost during the spring cast (D_{CAST}) was estimated from site-specific changes in the
202 proportion of individuals carrying an old lamina (P_{OB}) between successive sampling events
203 (i.e. winter to spring and spring to summer) multiplied by site-specific kelp density (D) and
204 the individual biomass of old lamina (B_{LAM}) to obtain daily losses in g FW m^{-2} between
205 sampling events:

206 $$D_{CAST} = P_{OB} \times D \times B_{LAM} \times t^{-1} \quad \text{Eq. 7}$$

207 where t is the time elapsed between two succeeding sampling events. Units of FW were
208 finally converted to units of carbon applying a DW:FW ratio of 0.163 ± 0.047 for blades and
209 0.135 ± 0.019 for stipes, respectively, and a C-content of 33.0 ± 3.1% of DW for blades and
210 29.7 ± 2.6% of DW for stipes (own unpublished values for this species, n = 32).
211
212 **Comparing detrital C-flux from L. kelp to that of other habitats.** We compared finally the
213 obtained values of detrital C donation by *L. hyperborea* to that of other terrestrial and coastal
214 habitats by using data obtained from the literature. Terrestrial habitats included temperate and
215 tropical forests and shrubs, temperate and tropical grass lands while coastal habitats included
216 marine phytoplankton, non-kelp seaweeds, seagrasses, mangroves and marshes. The

particulate detrital carbon donation included all types of litter-fall and detritus (e.g. leaves, branches and twigs, reproductive structures), but in most cases not below-ground detritus production. Numbers and references are in Supporting Information Table S1.

Statistical analyses. All values in the text are means ± 95% CI unless otherwise stated. Mean and maximum *REI* were compared across sites and seasons using two factor ANOVA. Normality of the residuals was tested by Kolmogorov-Smirnoff test and homogeneity of variances was tested by Levenes test. Most data (i.e. REI, kelp density, individual biomass, biomass per unit area, blade growth, blade erosion, dislodgment of plants and loss of old blades) did not meet the assumptions for parametric analysis (especially homogeneity of variance) and were therefore compared across sites and seasons using non-parametric repeated measures ANOVA (i.e. Friedman's test). Means were first compared across sites using season as a blocking factor, then compared across seasons using site as blocking factor. Multiple pair-wise comparisons were conducted using the Tukey procedure for ranked data when the Friedman test provided significant results (Zar 1999). Correlations between net production, blade erosion, dislodgment and relative wave exposure level (*REI*) were tested using non-parametric Spearman Rank Correlation analysis. The detritus production in different ecosystem types were compared using one way ANOVA. All tests were performed using $\alpha = 0.05$.

RESULTS

Temperature, light and relative wave exposure.

Water temperature averaged 7.1 ± 2.3°C (± sd) and ranged from 4.2°C in spring (March-April) to 11.5°C in late summer (August) (Fig. 2A). Daily light intensity reaching the canopy averaged 765 ± 855 lux (± sd) and ranged from 0 lux d^{-1} in December and January to 3877 lux

d^{-1} late June (Fig. 2B). Wind speed (Fig. 2C) averaged 6.5 ± 4.0 m sec^{-1} (± sd) and ranged from an average of 4 m sec^{-1} in summer to 8 m sec^{-1} in winter while maximum wind speed ranged from 18 m sec^{-1} in autumn to 26 and 32 m sec^{-1} in winter and spring, respectively. Mean and maximum wave exposure level (*REI*) varied between seasons and sites (Fig. 3A and 3B). Mean *REI* varied 10 to 25-fold between sites depending on season ($\chi^2_{r,4,10}$ = 33.4; p < 0.001) and was significantly higher at sites 1 - 5 than at sites 6 - 10. Maximum *REI* followed largely the same pattern across sites ($\chi^2_{r,4,10}$ = 33.8; p < 0.001), but the variation was larger than for mean *REI* (30 to 53-fold variation depending on season). Mean *REI* was highest during winter and lowest in autumn ($\chi^2_{r,4,10}$ = 13.3; p = 0.004), while maximum *REI* was highest in winter and lowest in summer ($\chi^2_{r,4,10}$ = 18.8; p < 0.001). Mean *REI* varied 1.6 to 2.8-fold between seasons (depending on site) while maximum *REI* varied 1.1 to 2.7-fold between seasons. Seasonal variation in *REI* was not consistent across all sites since some sites had larger seasonal variations in *REI* than others. This was likely due to seasonal variation in the dominant wind direction and showed that location and, thus, weighted effective fetch, played an important role for *REI*.

Individual plant traits. Individual kelp biomass (i.e. stipe plus lamina) averaged 48.2 ± 12.9 g C (± sd) and ranged from 24.0 to 77.0 g C depending on site and season (Fig. 4A). Individual stipe biomass (mean ± sd = 19.2 ± 6.8 g C) was larger at sites 5, 6 and 7 than at the remaining sites (26.6 *vs.* 16.0 g C; $\chi^2_{r,10,4}$ = 28.0; p < 0.001), but did not vary seasonally ($\chi^2_{r,4,10}$ = 6.2; p = 0.188). Individual blade biomass (mean ± sd = 29.0 ± 8.6 g C; Fig. 4B) was larger in plants from sites 1 to 6 than from sites 7 to 10 (32.8 *vs.* 23.3 g C $kelp^{-1}$; $\chi^2_{r,10,4}$ = 24.4; p = 0.004). Individual blade biomass was the only morphological variable that was correlated with *REI* (Spearman rank's R = 0.745; p = 0.013). Blade biomass was lowest in late winter and largest in summer (22.9 *vs.* 33.8 g C; $\chi^2_{r,4,10}$ = 16.6; p = 0.002). New blades

267 were initiated in early winter and increased in size during spring to reach maximum size in
268 August. Old, fully grown blades lost 35.8 ± 18.6 % of their biomass through erosion and
269 pruning between late summer and the following spring where they were cast.
270
271 **Kelp density, biomass and productivity.** Kelp density averaged 16.6 ± 1.3 (± sd) individuals
272 m^{-2} across sites and seasons (Figs. 5A and 5B). Density did not differ among sites ($\chi^2_{r,10,4}$ =
273 13.9; p = 0.126), but decreased slightly over the course of the study ($\chi^2_{r,4,10}$ = 12.8; p = 0.012;
274 density in August 2016 being higher than in March, May and August 2017; all p < 0.015).
275 Total kelp biomass per unit area averaged 770 ± 100 g C m^{-2} (± sd) across all sites
276 and sampling dates (Figs. 5C and 5D). Total biomass was higher at sites 3, 5, 6, 7 and 8 than
277 at the remaining sites (888 *vs.* 652 g C m^{-2}; $\chi^2_{r,10,4}$ = 20.4; p = 0.015). Total stipe biomass per
278 unit area averaged 313 ± 69 g C m^{-2} (± sd) across sites and sampling events, corresponding to
279 ca. 41% of the total biomass. Stipe biomass was higher at sites 5 to 8 than at the other sites
280 (415 *vs.* 245 g C m^{-2}; $\chi^2_{r,10,4}$ = 28.3; p < 0.001), but did not vary seasonally ($\chi^2_{r,4,10}$ = 6.6; p =
281 0.161). Total blade biomass per unit area averaged 458 ± 64 (± sd) g C m^{-2} and was similar
282 across sites, except for site 3 where it was higher than at all other sites ($\chi^2_{r,10,4}$= 17.4; p =
283 0.043). Blade biomass varied seasonally ($\chi^2_{r,4,10}$ = 13.0; p = 0.011), being lowest in late
284 winter (March) when the new blades were small and the old ones were heavily eroded, and
285 highest in late summer.
286 Daily blade production per unit area averaged 1.16 ± 0.11 g C m^{-2} (Fig. 5E and F)
287 and did not differ across sites ($\chi^2_{r,10,4}$ = 5.2; p = 0.813), but was much higher in spring than in
288 other seasons (3.24 ± 0.51 *vs.* 0.06 ± 0.04 to 0.99 ± 0.12 g C m^{-2} d^{-1}; $\chi^2_{r,3,10}$ = 26.0; p < 0.001).
289 Blade production was not correlated to *REI* (R = -0.248, p = 0.489). Annual blade production
290 (August 2016 to August 2017) amounted to 426.2 ± 39.4 g C m^{-2}, with more than 90% of that
291 taking place within 3 - 4 months in spring. The annual production of stipe biomass amounted

292 to 73.1 ± 16.2 g C m^{-2} yielding a total average productivity of 499.4 ± 49.9 g C m^{-2} y^{-1} across
293 the ten study sites.
294
295 **Detritus production.** Erosion losses per unit area averaged 0.29 ± 0.05 g C m^{-2} d^{-1} (Fig. 6A
296 and 6B) and did not differ across sites ($\chi^2_{r,10,4}$ = 3.5; p = 0.939) but differed between seasons,
297 ranging from 0.05 ± 0.05 g C m^{-2} d^{-1} in spring to 0.61 ± 0.22 g C m^{-2} d^{-1} in late summer
298 ($\chi^2_{r,3,10}$ = 25.6; p < 0.001).
299 Erosion losses were not correlated to *REI* (R = 0.006, p = 0.987). Annual biomass losses
300 through erosion amounted to 108.0 ± 7.2 g C m^{-2}.
301 The number of kelp plants or whole blades lost through dislodgment averaged 18.6 ±
302 10.8% $year^{-1}$ (data not shown) corresponding to an average biomass loss of 0.33 ± 0.19 g C m^{-2}
303 d^{-1} (Fig. 6C and D). Losses through dislodgement did not differ among sites ($\chi^2_{r,10,4}$ = 7.0; p
304 = 0.638), were not correlated to *REI* (R = -0.430, p = 0.214) and did not vary seasonally
305 ($\chi^2_{r,3,10}$ = 1.4; p = 0.711). Annual losses through dislodgment reached 114.5 ± 51.9 g C m^{-2} of
306 which 46% was made up by stipe material while the remaining 54% was blade material.
307 More than 99% of the plants collected during late winter (March 2017) had an old
308 blade attached to the distal end of their new blade, but this number fell to 37% in late May
309 2017. Most of the plants carrying an old blade in May lost them during our processing, so we
310 assume that these would have been lost within days in the field. None of the plants sampled in
311 August 2016 and 2017 carried an old blade. The spring cast of old blades corresponded to an
312 average biomass loss of 255.5 ± 43.2 g C m^{-2} y^{-1} (Fig. 6E; no difference across sites: $\chi^2_{r,10,4}$ =
313 5.4; p = 0.803) with the majority being lost between late March and early May (Fig. 6F).
314 The total production of detritus from *L. hyperborea* averaged 478.0 ±40.5 g C m^{-2} y^{-1}
315 across the ten study sites. Formation of blade detritus through dislodgment and blade erosion
316 was the least important form of detritus production, accounting for 24% and 23% of the total

317 detritus production, respectively, while the spring cast of old blades represented 53% of the
318 total detritus production (Fig. 7).
319
320
321 **DISCUSSION**
322 Our study confirmed that high latitude kelp forests in Norway are very productive and deliver
323 large amounts of particulate detritus that, depending on its form and timing of delivery, may
324 support secondary production and/or contribute to Blue Carbon through permanent burial in
325 marine sediments in deeper adjacent areas. The annual production of detritus from *Laminaria*
326 *hyperborea* (478 g C m^{-2}) was higher than that reported from southern England (202 g C m^{-2}),
327 but comparable to that found in northern Scotland (432 g C m^{-2}; Pessarrodona et al. 2018).
328 The study by Pessarrodona et al. (2018) is the only other one that reports rates of detritus
329 production for *L. hyperborea*. However, grazing on live *L. hyperborea* is usually low
330 (typically <10% of the biomass production; Norderhaug & Christie 2011) and the formation
331 of detritus can therefore be inferred from the annual production of biomass. The observed
332 production in this study (499 g C m^{-2} y^{-1}) is within the range of that reported for *L.*
333 *hyperborea* along the west coast of Norway, Isle of Man (UK), Helgoland (Germany) and
334 Normandy (France) (range: 376-825 g C m^{-2} y^{-1}; Lüning 1969, Jupp & Drew 1974, Sheppard
335 et al. 1978, Sjøtun et al. 1995, Pedersen et al. 2012), but higher than that reported from
336 Iceland and Finmark in northernmost Norway (ca. 250 g C m^{-2} y^{-1}; Gunnarsson 1991, Sjøtun
337 et al. 1993). The production of detritus from *L. hyperborea* seems thus to range from ca. 225
338 to ca. 750 g C m^{-2} y^{-1} (assuming grazing losses ~10% of NPP) across its distributional range,
339 which is similar to the production of detritus in other kelp species (table 1 in Krumhansl &
340 Scheibling 2012). The production of detrital C from *L. hyperborea* included only particulate
341 detritus (POC), but part of the C fixed in kelp photosynthesis is released as dissolved organic

342 C (DOC), which may support pelagic microorganisms (e.g. Newell et al. 1982) or contribute
343 to C-sequestration if transported below the mixed zone of the ocean (Krause-Jensen & Duarte
344 2016). Large uncertainties remain regarding the total production and fate of DOC from kelps,
345 but the DOC released from kelps appears to range from 14 to 34% of total the production
346 (POC plus DOC) depending on species and location (e.g. Newell et al. 1980, Abdullah &
347 Fredriksen 2004, Reed et al. 2015), which would represent an important component of detrital
348 production.
349 The processes through which kelp detritus is produced have implications for its
350 transfer to other habitats and its turn-over through consumption and decomposition. More
351 than 75% of the detritus formed by *L. hyperborea* was delivered as coarse material formed
352 through dislodgement of whole plants or the spring cast of old blades, while the rest was
353 delivered as smaller particles and small blade fragments through erosion. This compares to
354 the proportions reported by Pessarrodona et al. (2018) for this species. The large proportion of
355 coarse detritus is comparable to that found in *Macrocystis pyrifera* where dislodgement
356 account for almost 80% of the annual detritus production (Gerard 1976), but contrasts the
357 pattern found in *Ecklonia radiata* where most (78%) detritus is formed through erosion (de
358 Bettignies et al. 2013b). These inter-specific variations may be due to difference in
359 morphology since the thallus of *M. pyrifera* extends 10s of meters and forms floating
360 canopies that are susceptible to wave forces (Seymour et al. 1989, Graham et al. 1997),
361 whereas *E. radiata* is much shorter with scouring canopies that may stimulate erosion rate.
362 The morphology of *L. hyperborea* is intermediate between these extremes; it has a longer
363 stipe than *E. radiata* and no floating canopy like *M. pyrifera* so scouring and drag forces may
364 be less important.
365 Water motion is often considered a major driver for the formation of kelp detritus.
366 Blade erosion may be stimulated by water motion, although weakening of the blade tissue by

367 formation of sori, grazing and encrustation by bryozoans can also play a role (Krumhansl &
368 Scheibling 2011b, de Bettignies et al. 2012, Mohring et al. 2012). Erosion is correlated to
369 water motion in some species (e.g. *Laminaria digitata*; Krumhansl & Scheibling 2011a), but
370 not in others (e.g. *Saccharina latissima*; Krumhansl & Scheibling 2011a, *E. radiata*; de
371 Bettignies et al. 2013b). Erosion rate in *L. hyperborea* was not correlated to *REI* when
372 compared across sites although maximum *REI* varied 30 – 53 fold, but varied instead
373 seasonally with fast erosion coinciding with high *REI* in autumn and winter. Winter season is
374 also the time where the blades get older and more fragile, which increases erosion rate. The
375 lack of correlation between erosion rate and *REI* when compared across sites suggests thus
376 that seasonal ageing of the blade is a more important driver of elevated erosion than water
377 motion per se. Storms may cause dislodgement of whole kelps or their blades (Ebeling et al.
378 1985, Seymor et al. 1989, Filbee-Dexter & Scheibling 2012) as may weakening of the stipe
379 by sea urchin grazing (de Bettignies et al. 2012), but dislodgement rate was neither correlated
380 to *REI* nor to sea urchin density when compared across sites or seasons. Dislodgement rates in
381 *L. hyperborea* were much lower than in *E. radiata* (18% y^{-1} *versus* 44 – 55% y^{-1}; de
382 Bettignies et al. 2013b) and did not undergo any clear seasonal variation although storm
383 events were more frequent and intense in autumn and winter (Fig. 2C). de Bettignies et al.
384 (2015) found the same in a study on *E. radiata* and explained the low effect of water motion
385 by small thallus size and, thus, reduced drag, in winter when wave exposure was highest (de
386 Bettignies et al. 2013a). The blade of *L. hyperborea* is also slightly smaller in winter than in
387 other seasons (Fig. 4B), but blade size was positively correlated to *REI* when compared across
388 sites, so reduced drag in winter can hardly explain the low importance of water motion in the
389 present study.

390 Most kelp detritus was delivered as coarse fragments, but these may be transformed
391 to smaller size before reaching recipient communities outside the kelp forest. Once dislodged

392 or cast, coarse detritus can break-up mechanically due to scouring or grazers can shred it into
393 smaller pieces or consume it and deliver the remains as fecal pellets. Such transformation is
394 important for the fate of the detritus because size may affect its susceptibility to consumers,
395 its dispersal capacity and its decomposition. Sea urchins feed intensively on coarse kelp
396 detritus. The density of sea urchins (mainly the green sea urchin *Strongylocentrotus*
397 *droebachiensis*) in the study area varied from 1 to 10 m^{-2} across sites and their consumption
398 of kelp detritus inside and in the vicinity of our the kelp forest sites corresponded to 60 - 65%
399 of the total detritus production (Filbee-Dexter et al. submitted). Green sea urchins fed kelp
400 defecate 50 - 70% of the consumed detritus as small undigested, but fragmented material with
401 approximately the same chemical composition as 'intact' kelp detritus (Mamalona & Pelletier
402 2005), which may support suspension and deposit feeders within and outside the kelp forest
403 (Duggins et al. 1989, Fredriksen 2003, Leclerc et al. 2013, McMeans et al. 2013, Gaillard et
404 al. 2017). However, the importance of kelp detritus as a food source has recently been
405 questioned by a review showing that trophic studies based on stable C-isotope data alone may
406 overestimate the trophic importance of kelp particles relative to that of phytoplankton (Miller
407 & Page 2012)
408 Detritus that is not mineralized by consumers within and near the kelp forests will be
409 prone to dispersal, decomposition or burial. Small kelp particles sink more slowly than larger
410 fragments, whole blades or stipes, which allow for a wider dispersal (Wernberg & Filbee-
411 Dexter 2018). Filbee-Dexter et al. (submitted) used sinking rates for different sized kelp
412 detritus and hydrodynamic modeling to simulate particle transport in the study area and found
413 that the median dispersal range of whole kelp blades was 8.5 km (maximum range = 150 km)
414 whereas it was 26 km (maximum >300 km) for small kelp particles. Beach cast of kelp is
415 often observed after storms (Griffiths et al. 1983, Seymor et al. 1989), but the coastline in the
416 study area is steep and we did not observe substantial accumulations of kelp detritus on the

417 shore. We hypothesize therefore that excess detritus is exported to the deeper parts in the area,
418 which is supported by trawl collections and video observations in the study area (Filbee-
419 Dexter et al. 2018). More than 50% of the kelp detritus was formed during the spring cast
420 between April and May, coinciding with observations of large amounts of coarse kelp detritus
421 within and around the kelp forests (Filbee-Dexter et al. 2018). Large amounts of coarse kelp
422 detritus were subsequently (late May) observed below the kelp forests at depths from 20 to 80
423 m and in the deepest portions of the study area (~ 400 m) confirming that the detritus was
424 exported several kilometers away from the source populations within days to weeks of its
425 formation. The amount of visible kelp detritus was much lower and the fragments smaller in
426 August, indicating that continuous fragmentation and transport to deeper sites in the study
427 area occurred during summer.
428 Kelp detritus that is not consumed will ultimately decompose or become buried in
429 deeper areas. Laboratory studies show that coarse detritus from *L. hyperborea* loses more than
430 40% of its initial C-biomass within 3 - 4 weeks and decomposes completely in less than one
431 year under aerobic conditions, while decomposition under anoxic conditions (such as in
432 deeper areas) stops after 5-6 months leaving 20 - 25% of the initial biomass to decompose at
433 extremely low rates or not at all (Frisk 2017). Decomposition rate depends also on particle
434 size. Fecal pellets from sea urchins fed with kelp detritus lose almost 80% of their initial C-
435 mass in two weeks (Sauchyn & Scheibling 2009), which is much faster than for larger kelp
436 fragments. Decomposition of kelp detritus can thus be fast depending on the environmental
437 conditions and the degree of fragmentation, while burial of significant quantities of kelp C
438 requires rapid export to areas where the conditions disfavor mineralization through
439 consumption or decomposition.
440 The potential export of detrital kelp C to the non-vegetated portions of the study area
441 can be estimated from the production of kelp detritus per unit area and kelp coverage in the

area. Kelp covered ca. 22 km^2 of the 126 km^2 covered by ocean in the study area (Fig. 1). The total production of kelp detritus in the study area amounts to 10517 T C y^{-1} or 101 g C m^{-2} y^{-1} if dispersed evenly over the 104 km^2 of non-vegetated area and assuming no consumption and decomposition. The potential input of detrital kelp C is comparable to the vertical flux of POC (marine snow) from the pelagic zone, which ranges from 93 to 150 g C m^{-2} y^{-1} in the outer part of Malangen Fjord (Keck & Wassmann 1996). Kelp detritus may thus contribute significantly to the total input of C to the deeper portions of the study area, although the input must be is less than estimated above when consumption by sea urchins and rapid initial decomposition are taken into account.

The importance of Blue C has lately received increased attention (Mcleod et al. 2011, Duarte 2017, Raven 2017) and coastal habitats such as mangroves, marshlands and seagrasses are now recognized as significant C-sinks (Chmura et al. 2003, Donato et al. 2011, Fourqurean et al. 2012), while the role of kelps and other macroalgae is still being debated (Howard et al. 2017, Krause Jensen et al. 2018, Smale et al. 2018). Quantifying the formation of kelp detritus is a first, but important step when evaluating the potential role of kelps as donors to C-sequestration. The production of detrital C by *L. hyperborea* reported here (~ 500 g C m^{-2} y^{-1}) is well within the range of that in other kelps, seagrasses, and mangroves, but significantly lower than marshes and significantly higher than marine phytoplankton, non-kelp seaweeds and terrestrial habitats such as forests and grasslands (Fig. 8, one way ANOVA: $F_{7,488} = 13.8$, $p < 0.001$; Suppl. information Table 1). The substantial production of detrital C from kelp forests suggests that kelp systems could play an important role as Blue C-donors to marine sediments. However, most of the studies on detritus production in grasslands, forests, mangroves and marshes report only above-ground litter fall and do not include below-ground production of detritus, which means the numbers from these systems may be under-estimated.

Blue C is defined as the sequestration of C from marine organisms that takes place when burial rates in sediments exceed long-term rates of erosion and decomposition. The importance for Blue C depends therefore not only on the amount of detrital C being produced, but also on re-mineralization of C through consumption by detritivores and/or through decomposition, which will determine how much of the C can be buried. Kelps usually grow on hard substrates and do not have below-ground tissues like seagrasses, mangrove trees and marsh plants. Thus export of kelp detritus to marine sediments where the conditions disfavor consumption and/or decomposition plays an important role in the final fate of kelp C. Future studies should focus on the different fates of kelp detritus and explore how much is consumed, how much is exported to potential Blue C sediments and how fast and under which environmental conditions detrital C is re-mineralized through decomposition.

Acknowledgements

This study was funded by the Norwegian Research Council through the KELPEX project (NRC grant no. 255085) and TW's participation was further supported by the Australian Research Council (DP160100114). We like to thank Sabine Popp, Eva Ramirez-Llodra, Amanda Poste, and Hjalte Hjarlgaard Hansen for valuable help with some of the field-work at Sommarøy and two anonymous reviewers for valuable comments to an earlier version of this manuscript.

489 **LITERATURE CITED**

490 Abdullah MI, Fredriksen S (2004) Production, respiration and exudation of dissolved organic
491 matter by the kelp *Laminaria hyperborea* along the west coast of Norway. J Mar Biol
492 Assoc UK 84: 887−894.

493 Bekkby T, Moy FE, Olsen H, Rinde E, Bodvin T, Bøe R, Steen H, Grefsrud ES, Espeland SH,
494 Pedersen A, Jørgensen NM (2013) The Norwegian Programme for Mapping of Marine
495 Habitats - Providing Knowledge and Maps for ICZMP. In: Moksness E, Dahl E,
496 Støttrup J (eds) Global Challenges in Integrated Coastal Zone Management Vol II. John
497 Wiley & Sons Ltd. Oxford, UK.

498 Carr MH, Neigel JE, Estes JA, Andelman S, Warner RR, Largier JL (2003) Comparing
499 marine and terrestrial ecosystems: Implications for the design of coastal marine reserves.
500 Ecol Appl 13: 90 – 107

501 Cebrian J (1999) Patterns in the fate of production in plant communities. Am Nat 154: 449–
502 468, doi:10.1086/303244.

503 Chmura GL, Anisfeld SC, Cahoon DR, Lynch JC (2003) Global carbon sequestration in tidal,
504 saline wetland soils. Global Biogeochem Cy 17: 1-11. doi: 10.1029/2002GB001917.

505 Colombini I, Chelazzi L (2003) Influence of marine allochthonous input on sandy beach
506 communities. Oceanogr Mar Biol 41: 115–159, doi:10.1201/9780203180570.ch3.

507 Davies CE, Moss D (2003) EUNIS habitat classification. European Topic Centre on Nature
508 Protection and Bio-diversity, Paris. http://eunis.eea.europa.eu/habitats.jsp

509 de Bettignies T, Thomsen MS, Wernberg T (2012) Wounded kelps: Patterns and
510 susceptibility to breakage. Aquat Biol 17: 223–233, doi:10.3354/ab00471.

511 de Bettignies T, Wernberg T, Lavery PS (2013a) Size, not morphology, determines
512 hydrodynamic performance of a kelp during peak flow. Mar Biol 160: 843–851,
513 doi:10.1007/s00227-012-2138-8.

514 de Bettignies T, Wernberg T, Lavery PS, Vanderklift MA, Mohring MB (2013b) Contrasting
515 mechanisms of dislodgement and erosion contribute to production of kelp detritus.
516 Limnol Oceanogr 58: 1680–1688, doi:10.4319/lo.2013.58.5.1680.
517 de Bettignies T, Wernberg T, Lavery PS, Vanderklift MA, Gunson JR, Symonds G, Collier N
518 (2015) Phenological decoupling of mortality from wave forcing in kelp beds. Ecology
519 96: 850-861.
520 Donato DC, Kaufmann JB, Murdiyarso D, Kurnianto S, Stidham M, Kanninen M (2011)
521 Mangroves among the most carbon-rich forests in the tropics. Nat Geosci 4: 293-297.
522 Duarte CM (2017) Hidden forests, the role of vegetated coastal habitats in the ocean carbon
523 budget. Biogeosciences 14: 301–310. doi:10.5194/bg-14-301-2017.
524 Duggins D, Simenstad C, Estes J (1989) Magnification of secondary production by kelp
525 detritus in coastal marine ecosystems. Science 245: 170–173.
526 Ebeling AW, Laur DR, Rowley RJ (1985) Severe storm disturbances and reversal of
527 community structure in a southern California kelp forest. Mar Biol 84: 287−294.
528 Filbee-Dexter K, Scheibling RE (2012) Hurricane-mediated defoliation of kelp beds and
529 pulsed delivery of kelp detritus to offshore sedimentary habitats. Mar Ecol Prog Ser
530 455: 51–64, doi: 10.3354/meps09667.
531 Filbee-Dexter K, Scheibling RE (2016) Spatial patterns and predictors of drift algal subsidy in
532 deep subtidal environments. Estuaries and Coasts 39: 1724–1734, doi: 10.1007/s12237-
533 016-0101-5.
534 Filbee-Dexter K, Wernberg T, Norderhaug KM, Ramirez-Llodra E, Pedersen MF (2018)
535 Movement of pulsed resource subsidies from kelp forests to deep fjords. Oecologia 187:
536 291–304, doi: 10.1007/s00442-018-4121-7.
537 Filbee-Dexter K, Pedersen MF, Fredriksen S, Norderhaug KM, Rinde E, Kristiansen T,
538 Albretsen J, Wernberg T (accepted for publication) Carbon export is facilitated by

539 marine shredders transforming kelp detritus. Oecologia.
540 Fonseca MS, Bell SS (1998). Influence of physical setting on seagrass landscapes near
541 Beaufort, North Carolina, USA. Mar Ecol Prog Ser 171: 109-121.
542 Fourqurean JW, Duarte CM, Kennedy H, Marbà N, Holmer M, Mateo MA, Apostolaki ET,
543 Kendrick GA, Krause-Jensen, McGlathery KJ, Serrano O (2012) Seagrass ecosystems
544 as a globally significant carbon stock. Nat Geosci 5: 505-509. doi: 10.1038/NGEO1477.
545 Fredriksen S (2003) Food web studies in a Norwegian kelp forest based on stable isotope (^{13}C
546 and ^{15}N) analysis. Mar Ecol Prog Ser 260: 71−81.
547 Frisk NL (2017) The effect of temperature and oxygen availability on decay rate and changes
548 in food quality of *Laminaria hyperborea* detritus. Master thesis, Department of Science
549 and Environment, Roskilde University, Denmark.
550 Gaillard B, Meziane T, Tremblay R, Archambault P, Blicher ME, Chauvaud L, Rysgaard S,
551 Olivier F (2017) Food resources of the bivalve *Astarte elliptica* in a sub-Arctic fjord: a
552 multi-biomarker approach. Mar Ecol Prog Ser 567: 139–156, doi:10.3354/meps12036
553 Gerard VA (1976) Some aspects of material dynamics and energy flow in a kelp forest in
554 Monterey Bay, California. PhD dissertation, University of California, Santa Cruz, USA.
555 Graham MH, Harrold C, Lisin S, Light K, Watanabe JM, Foster MS (1997) Population
556 dynamics of giant kelp *Macrocystis pyrifera* along a wave exposure gradient. Mar Ecol
557 Prog Ser 148: 269–279.
558 Griffiths CL, Stenton-Dozey J, Koop K (1983) Kelp wrack and the flow of energy through a
559 sandy beach ecosystem. In: McLachlan A, Erasmus T (eds) Sandy beaches as
560 ecosystems. W. Junk Publishers, The Hague, p. 547−556.
561 Gunnarsson K (1991) Populations de *Laminaria hyperborea* et *Laminaria digitata*
562 (Phéophycées) dans la baie de Breidifjördur, Islande. Rit Fiskideildar. J Mar Res Inst
563 Reykjavik 12:1−148.

564 Howard J, Sutton-Grier A, Herr D, Kleypas J, Landis E, Mcleod E, Pigeon E, Simpson S
565 (2017) Clarifying the role of coastal and marine systems in climate mitigation. Front
566 Ecol Environ 15: 42-50. doi: 10.1002/fee.1451.
567 Jupp BP, Drew EA (1974) Studies on the growth of *Laminaria hyperborea* (Gunn) Fosl. I.
568 Biomass and productivity. J Exp Mar Biol Ecol 15: 185−196
569 Ince R, Hyndes GA, Lavery PS, Vanderklift MA (2007) Marine macrophytes directly
570 enhance abundances of sandy beach fauna through provision of food and habitat.
571 Estuarine, Coastal and Shelf Science, 74: 77-86.
572 Keck A, Wassmann P (1996) Temporal and spatial patterns of sedimentation in the subarctic
573 fjord Malangen, northern Norway. Sarsia 80: 259-276.
574 Krause-Jensen D, Duarte CM (2016) Substantial role of macroalgae in marine carbon
575 sequestration. Nat Geosci 9: 737–742, doi: 10.1038/ngeo2790.
576 Krause-Jensen D, Lavery P, Serrano O, Marbà N, Masque P, Duarte CM (2018) Sequestration
577 of macroalgal carbon: the elephant in the Blue Carbon room. Biol Lett 14: 20180236,
578 doi.org/10.1098/rsbl.2018.0236.
579 Krumhansl KA, Scheibling RE (2011a) Detrital production in Nova Scotian kelp beds:
580 Patterns and processes. Mar Ecol Prog Ser 421: 67–82, doi:10.3354/meps08905
581 Krumhansl KA, Lee MJ, Scheibling RE (2011b) Grazing damage and encrustation by an
582 invasive bryozoan reduce the ability of kelps to withstand breakage by waves. J Exp
583 Mar Biol Ecol 407: 12−18.
584 Krumhansl KA, Scheibling RE (2012) Production and fate of kelp detritus. Mar Ecol Prog Ser
585 467: 281–302, doi:10.3354/meps09940
586 Leclerc J-C, Riera P, Leroux C, Lévêque L, Davoult D (2013) Temporal variation in organic
587 matter supply in kelp forests: linking structure to trophic function. Mar Ecol Prog Ser
588 494: 87-105

589 Lüning K (1969) Standing crop and leaf area index of the sublittoral *Laminaria* species near
590 Helgoland. Mar Biol 3: 282−286.
591 Mamelona J, Pelletier É (2005) Green urchin as a significant source of fecal particulate
592 organic matter within nearshore benthic ecosystems. J Exp Mar Bio Ecol 314: 163–174,
593 doi: 10.1016/J.JEMBE.2004.08.026.
594 Mann KH (1973) Seaweeds: Their productivity and strategy for growth. Science 182: 975–
595 981, doi:10.1126/science.182.4116.975.
596 McLeod E, Chmura GL, Bouillon S, Salm R, Björk M, Duarte CM, Lovelock CE, Schlesinger
597 WH, Silliman BR (2011) A blueprint for blue carbon: toward an improved
598 understanding of the role of vegetated coastal habitats in sequestering CO_2. Front Ecol
599 Environ 9: 552–560. doi:10.1890/110004.
600 McMeans BC, Rooney N, Arts MT, Fisk AT (2013) Food web structure of a coastal Arctic
601 marine ecosystem and implications for stability. Mar Ecol Prog Ser 482: 17-28, doi:
602 10.3354/meps10278.
603 Miller RJ, Page HM (2012) Kelp as a trophic resource for marine suspension feeders: a
604 review based on isotope-based evidence. Mar Biol 159: 1391-1402
605 Mohring MB, Wernberg T, Kendrick GA, Rule MJ (2012) Reproductive synchrony in a
606 habitat-forming kelp and its relationship with environmental conditions. Mar Biol 160:
607 119–126, doi:10.1007/s00227-012-2068-5.
608 Newell RC, Field JG, Griffiths CL (1982) Energy balance and significance of
609 microorganisms in a kelp bed community. Mar Ecol Prog Ser 8: 103-113.
610 Norderhaug KM, Christie H (2011) Secondary production in a *Laminaria hyperborea* kelp
611 forest and variation according to wave exposure. Est Coast Shelf Sci 95: 135-144.
612 Parke M (1948) Studies of British Laminariaceae. I. Growth in *Laminaria saccharina* (L.)
613 Lamour. J Mar Biol Ass UK 27: 651–709.

614 Pedersen MF, Nejrup LB, Fredriksen S, Christie H, Norderhaug KM (2012) Effects of wave
615 exposure on population structure, demography, biomass and productivity of the kelp
616 *Laminaria hyperborea*. Mar Ecol Prog Ser 451: 45−60.
617 Pessarrodona A, Moore PJ, Sayer MDJ, Smale DA (2018) Carbon assimilation and transfer
618 through kelp forests in the NE Atlantic is diminished under a warmer ocean climate.
619 Glob Change Biol 24: 4386-4398, doi: 10.1111/gcb.14303.
620 Polis GA, Anderson WB, Holt RD (1997) Toward an integration of landscape and food web
621 ecology: The dynamics of spatially subsidized food webs. Ann Rev Ecol Syst 28: 289–
622 316, doi:10.1146/annurev.ecolsys.28.1.289.
623 Poore AG, Campbell AH, Coleman RA, Edgar GJ, Jormalainen V, Reynolds PL, Sotka EE,
624 Stachowicz JJ, Taylor RB, Vanderklift MA, Duffy JE (2012) Global patterns in the
625 impact of marine herbivores on benthic primary producers. Ecol Lett 15: 912-922, doi:
626 10.1111/j.1461-0248.2012.01804.x.
627 Raven JA (2017) The possible role of algae in restricting the increase in atmospheric CO_2 and
628 global temperature. Eur J Phycol 52: 506–522. doi:10.1080/09670262.2017.1362593.
629 Reed DC, Carlson CA, Halewood ER, Nelson JC, Harrer SL, Rassweiler A, Miller RJ (2015)
630 Patterns and controls of reef-scale production of dissolved organic carbon by giant kelp
631 *Macrocystis pyrifera.* Limnol Oceanogr 60: 1996–2008.
632 Sauchyn L, Scheibling R (2009) Degradation of sea urchin feces in a rocky subtidal
633 ecosystem: implications for nutrient cycling and energy flow. Aquat Biol 6: 99–108,
634 doi: 10.3354/ab00171.
635 Seymour RJ, Tegner MJ, Dayton PK, Parnell PN (1989) Storm wave induced mortality of
636 giant kelp, *Macrocystis pyrifera*, in Southern California. Estuar Coast Shelf Sci 28:
637 277–292, doi:10.1016/0272-7714(89)90018-8.
638 Sheppard CRC, Jupp BP, Sheppard A, Bellamy DJ (1978) Studies on the Growth of

639 *Laminaria hyperborea* (Gunn.) Fosl. and *Laminaria ochroleuca* De La Pylaie on the
640 French Channel Coast. Bot Mar 21: 109-116. doi: 10.1515/botm.1978.21.2.109
641 Sjötun K, Fredriksen S, Lein TE, Rueness J, Sivertsen K (1993) Population studies of
642 *Laminaria hyperborea* from its northern range of distribution in Norway.
643 Hydrobiologia 260/261: 215-221.
644 Sjötun K, Fredriksen S, Rueness J, Lein TE (1995) Ecological studies of the kelp *Laminaria*
645 *hyperborea* (Gunnerus) Foslie in Norway. In: Skjoldal HR, Hopkins C, Erikstad KE,
646 Leinaas HP (eds) Ecology of fjords and coastal waters. Elsevier Science BV. Pp 525 –
647 536.
648 Smale DA, Burrows MT, Moore P, O'Connor N, Hawkins SJ (2013) Threats and knowledge
649 gaps for ecosystem services provided by kelp forests: a northeast Atlantic perspective.
650 Ecology and Evolution 3: 4016–4038.
651 Smale DA, Moore PJ, Queirós AM, Higgs ND, Burrows MT (2018) Appreciating
652 interconnectivity between habitats is key to blue carbon management. Front Ecol
653 Environ 16: 71-73. doi: 10.1002/fee.1765.
654 Steneck RS, Johnson CR (2013) Kelp Forests: Dynamic patterns, processes, and feedbacks. In
655 Bertness M, Silliman B, Stachowitz J (eds) Marine Community Ecology. pp 315–336.
656 Sinauer.
657 Tala F, Edding M (2005) Growth and loss of distal tissue in blades of *Lessonia nigrescens*
658 and *Lessonia trabeculata* (Laminariales). Aquat Bot 82: 39–54.
659 Vanderklift MA, Wernberg T (2008) Detached kelps from distant sources are a food subsidy
660 for sea urchins. Oecologia 157: 327–335, doi:10.1007/s00442-008-1061-7.
661 Vetter E, Dayton P (1999). Organic enrichment by macrophyte detritus, and abundance
662 patterns of megafaunal populations in submarine canyons. Mar Ecol Prog Ser 186: 137-
663 148.

664 Wernberg T, Vanderklift MA, How J, Lavery PS (2006) Export of detached macroalgae from
665 reefs to adjacent seagrass beds. Oecologia 147: 692–701, doi: 10.1007/s00442-005-
666 0318-7.
667 Wernberg T, Smale DA, Tuya F, Thomsen MS, Langlois TJ, de Bettignies T, Bennett S,
668 Rousseaux CS (2013) An extreme climatic event alters marine ecosystem structure in a
669 global biodiversity hotspot. Nat Clim Change 3: 78-82, doi: 10.1038/nclimate1627.
670 Wernberg T, Filbee-Dexter K (2018) Grazers extend blue carbon transfer by slowing sinking
671 speeds of kelp detritus. Scientific Reports 8: 17180, doi: 10.1038/s41598-018-34721-z.
672 Wernberg T, Krumhansl K, Filbee-Dexter K, Pedersen MF (2019) Status and trends for the
673 worlds kelp forests. In Sheppard C (ed) World Seas: An Environmental Evaluation Vol.
674 III: Ecological Issues and Environmental Impacts. pp 57–78, Elsevier.
675 Zar J (1999) Biostatistical Analysis. Prentice-Hall, Inc., NJ, USA, 929.
676

677 **Figure legends.**

678 **Fig. 1** Map of outer Malangen fjord with study sites 1-10. Light brown is land and blue is
679 ocean surface while modeled kelp areas are shown in green. Numbers refer to the sampling
680 sites

681 **Fig. 2** Seasonal variations (August 2016 to August 2017) in: (a) daily water temperature
682 (averaged across sites), (b) daily light intensity reaching the canopy (averaged across sites)
683 and (c) hourly measures of wind speed obtained from Hekkingen lighthouse

684 **Fig. 3** Relative wave exposure (*REI*) at all sites and seasons: (a) mean wave exposure and (b)
685 maximum wave exposure. Sites are ranked according to increasing wave exposure along the
686 x-axis. Values are means ± 95 CI (Aug – Oct: n = 69; Oct – March: n = 161; March – May: n
687 = 54; May – Aug: n = 60)

688 **Fig. 4** *Laminaria hyperborea* individual plant variables: (a) individual kelp biomass at the 10
689 study sites (averaged across seasons) (b) seasonal variation in individual kelp biomass
690 (averaged across sites). Sites are ranked according to increasing wave exposure level (*REI*)
691 along the x-axis. Mean values ±95% CI (Fig. 4a: n = 4; Fig. 4b: n = 10)

692 **Fig 5** *Laminaria hyperborea* biomass and productivity: (a) kelp density at the 10 study sites
693 (averaged across seasons), (b) seasonal variation in kelp density (averaged across sites), (c)
694 kelp biomass per unit area at the 10 study sites (averaged a cross seasons), (d) seasonal
695 variation in kelp biomass (averaged across sites), (e) blade production at each site in each of
696 four seasons and, (f) seasonal variation in average blade production (averaged across sites).
697 Sites are ranked according to increasing wave exposure level (*REI*) along the x-axis. Mean
698 values ±95% CI (Fig. 5a: n = 4; Fig. 5b: n = 10; Fig. 5c: n = 4; Fig. 5d: n = 10; Fig. 5e: n = 1;
699 Fig. 5f: n = 10)

Fig. 6 *Laminaria hyperborea* detritus production: (a) seasonal erosion rate at each site in each of four seasons, (b) seasonal variation in erosion rate (averaged across sites), (c) seasonal dislodgement at each site in each of four seasons, (d) seasonal variation in dislodgement rate (averaged across sites), (e) seasonal spring cast of old blades at each site in each of four seasons, and (f) seasonal variation in losses through spring cast of old blades (averaged across sites). Sites are ranked according to increasing wave exposure level (*REI*) along the x-axis. Mean values ±95% CI (Fig. 6a: n = 1; Fig. 6b: n = 10; Fig. 6c: n = 1; Fig. 6d: n = 10; Fig. 6e: n = 1; Fig. 6f: n = 10)

Fig. 7 Cumulated production of detritus through blade erosion, dislodgement and spring cast of old blades during autumn, winter, spring and summer (averaged across the 10 study sites). Mean values ±95% CI (n = 10)

Fig. 8. Annual per area production of detrital C in different habitats. The flow of C via detritus includes various kinds of litterfall and detritus production. One-way ANOVA revealed significant differences between habitats ($F_{7,488} = 13.8$, $p < 0.001$) and Dunnett's test was subsequently used to compare the detrital production of each habitat to that of kelps. Asterix indicate significant differences when compared to kelps (*: $p < 0.05$, **: $p < 0.01$, ns: non-significant). Details and references are provided in Supporting Information Table S1. Values are means ± 95% CI (n for each data set indicated on figure)

720

Figure 1

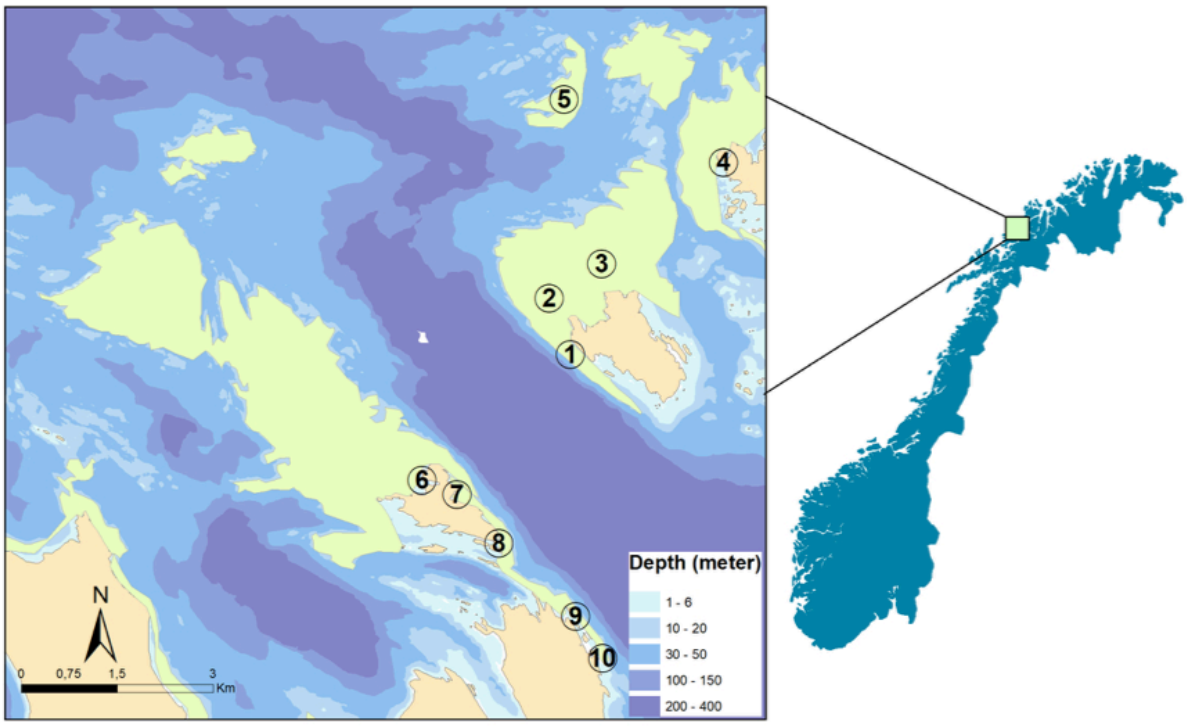

721

722 **Figure 2**

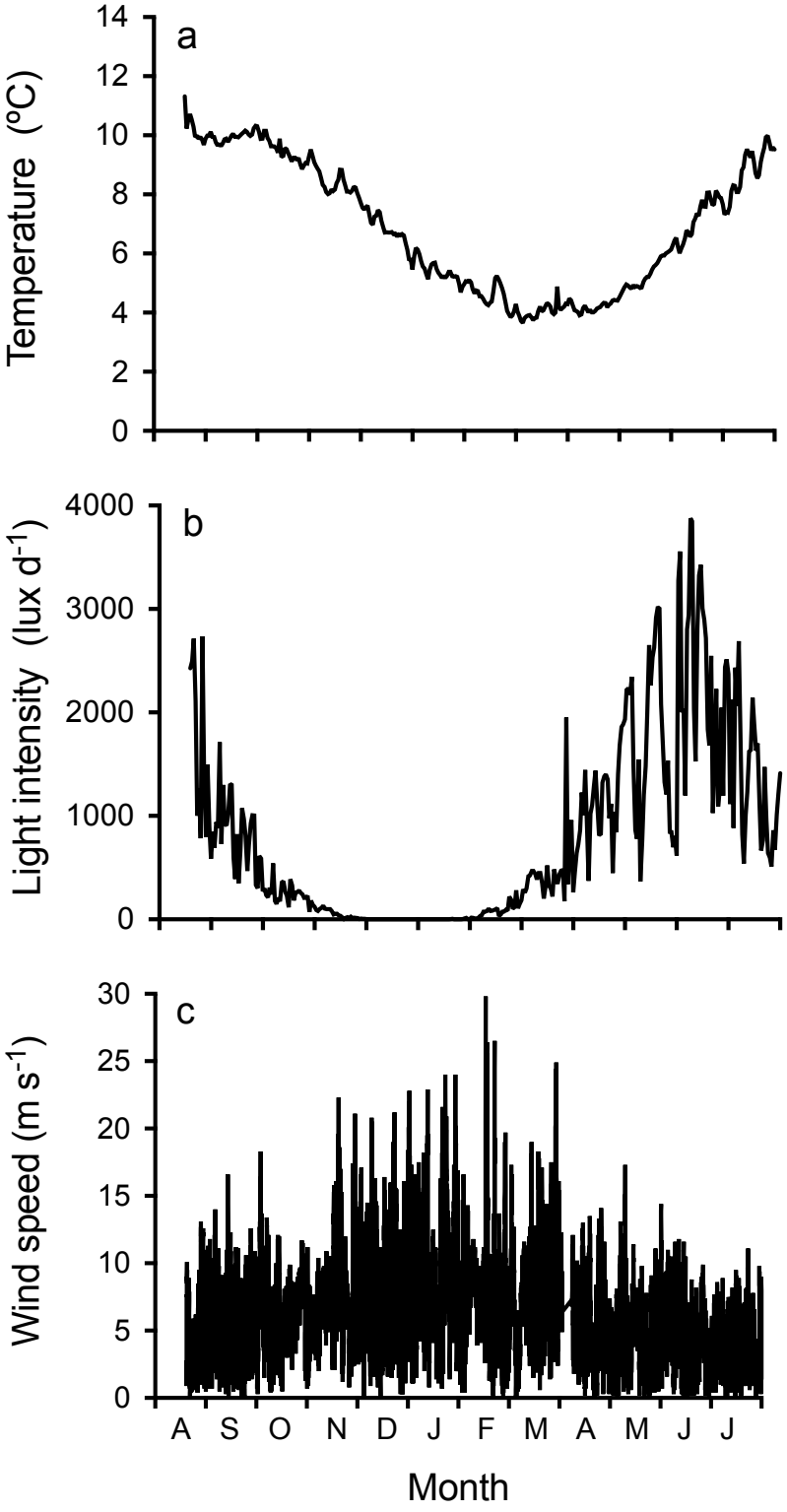

723

724

725 **Figure 3**

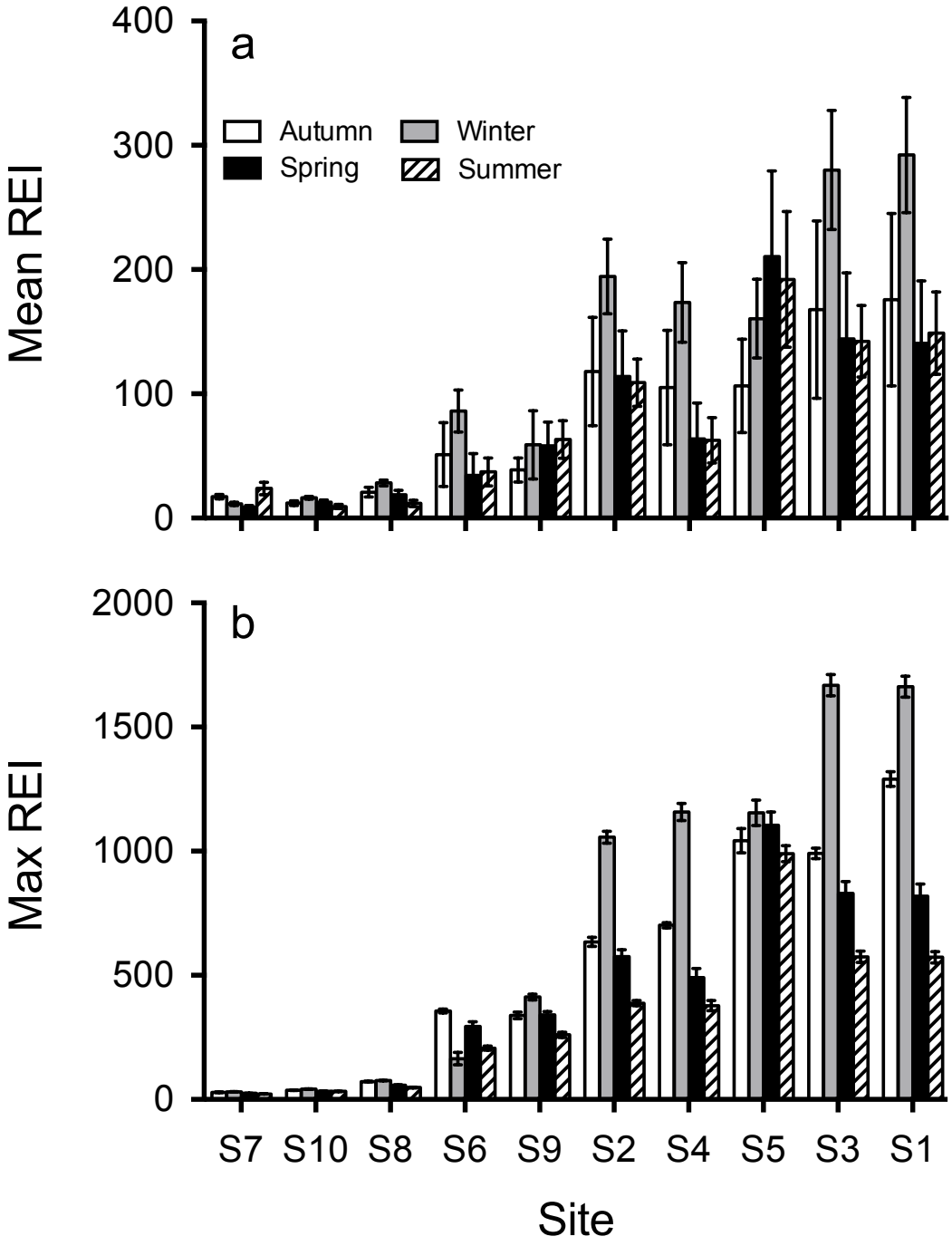

726

727

728 **Figure 4**

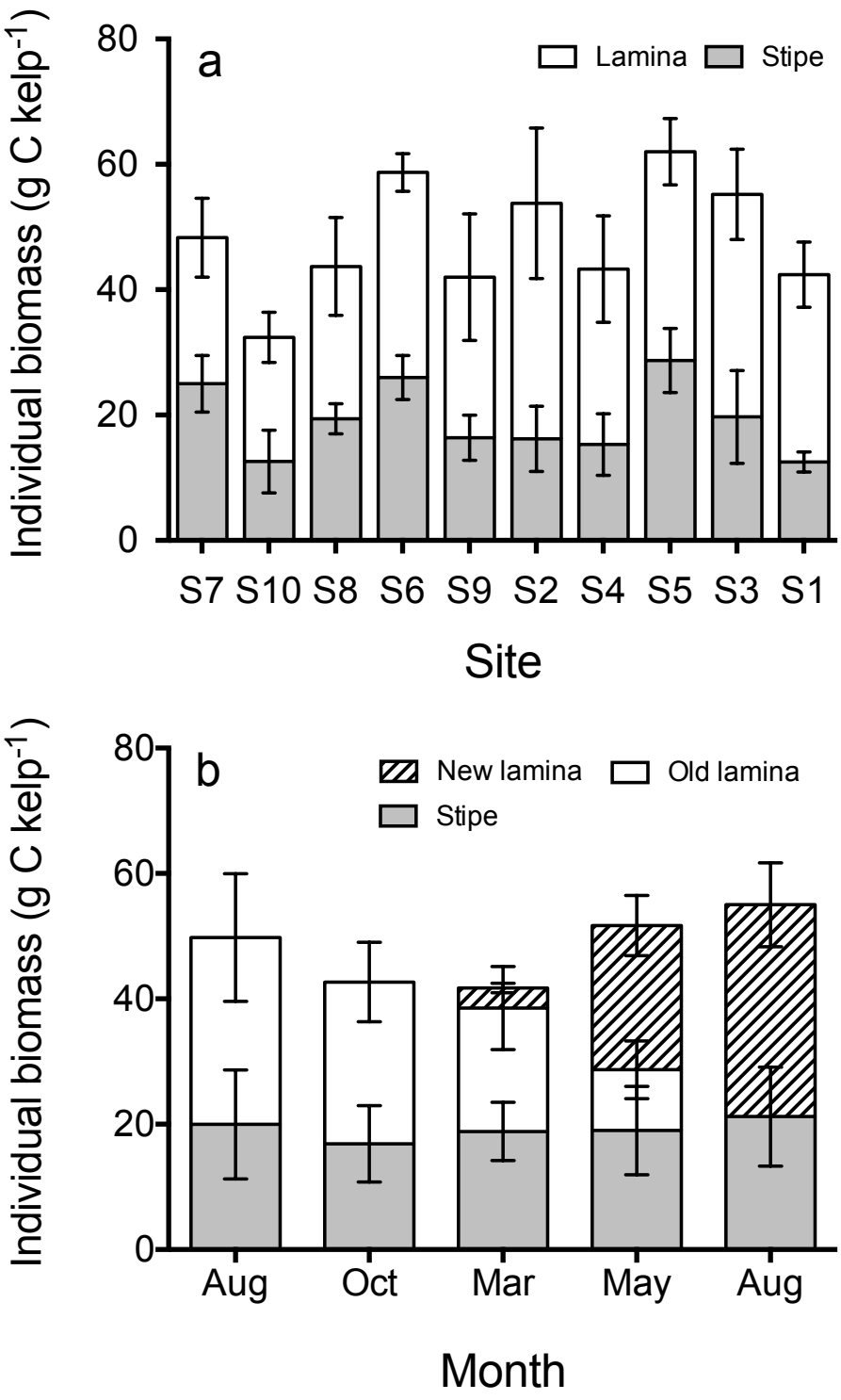

729

730

731 **Figure 5**

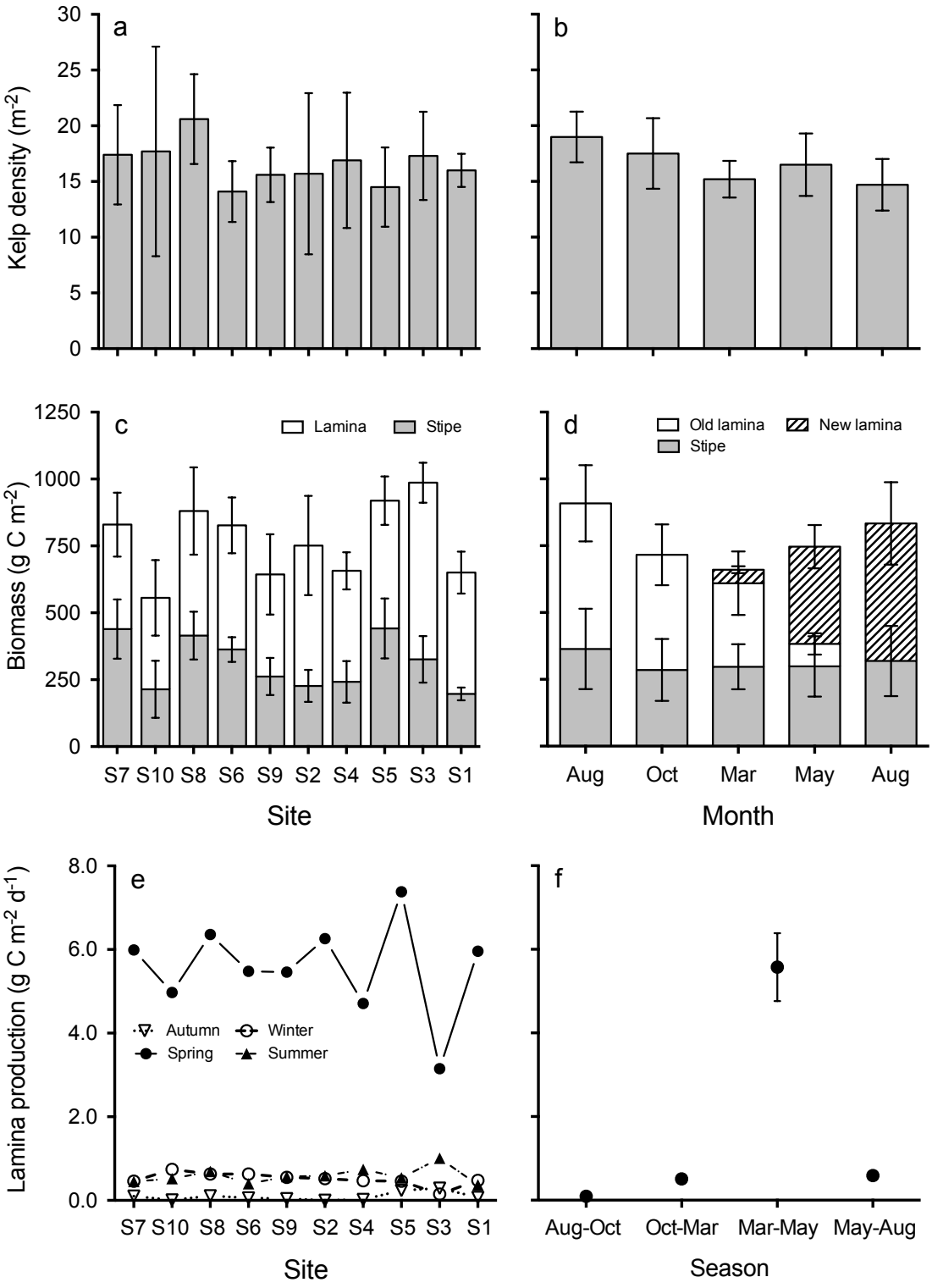

732

733

734 **Figure 6**

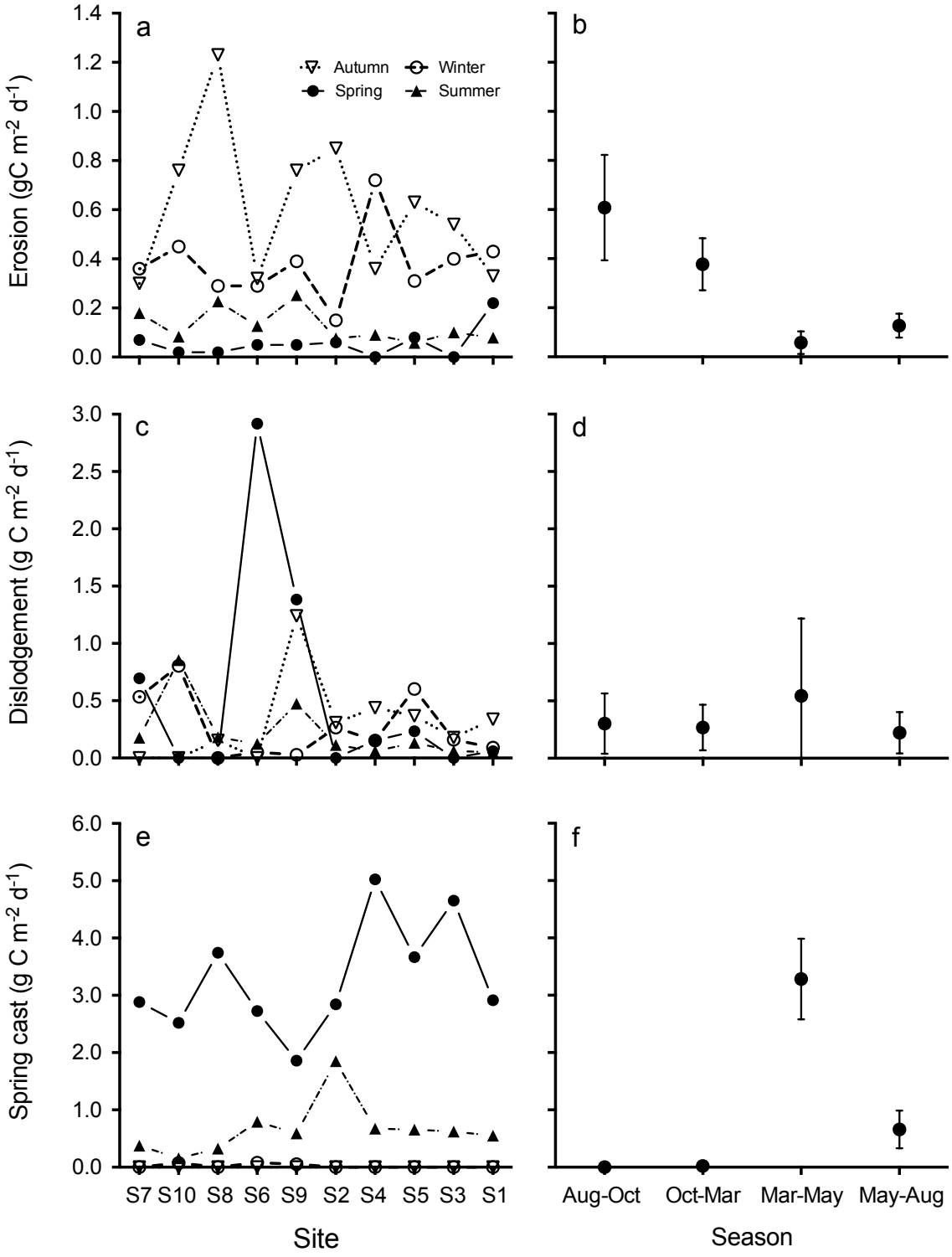

735

736

737

738 **Figure 7**

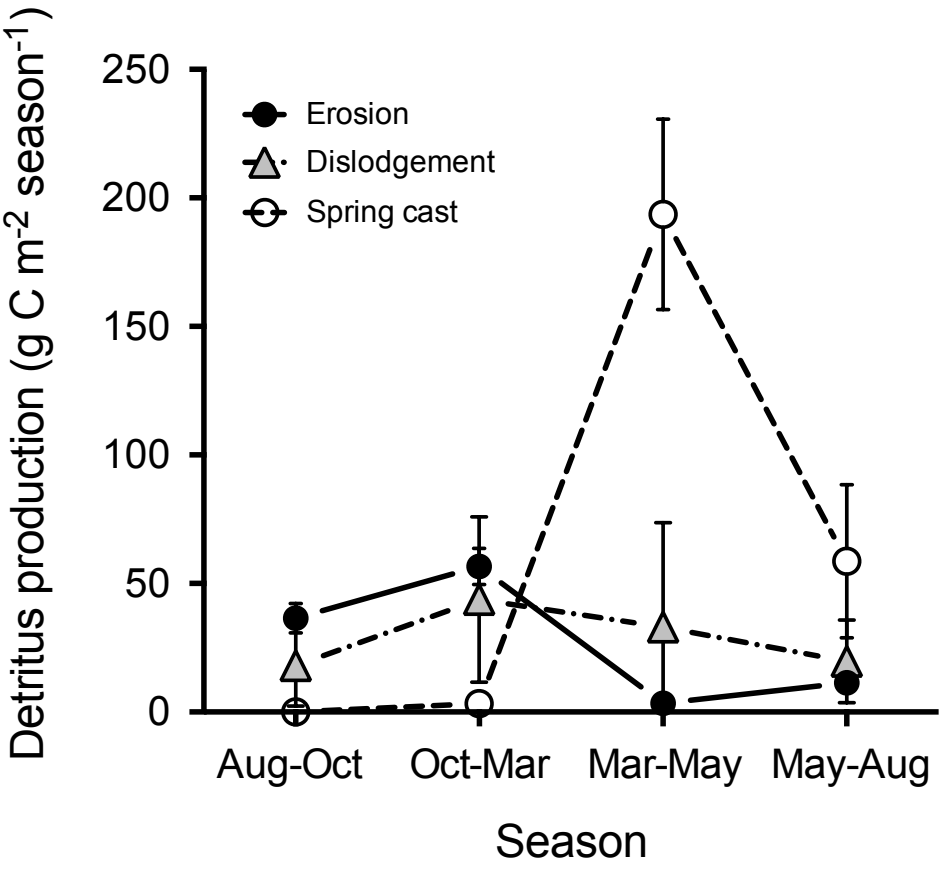

739

740

741 **Figure 8**

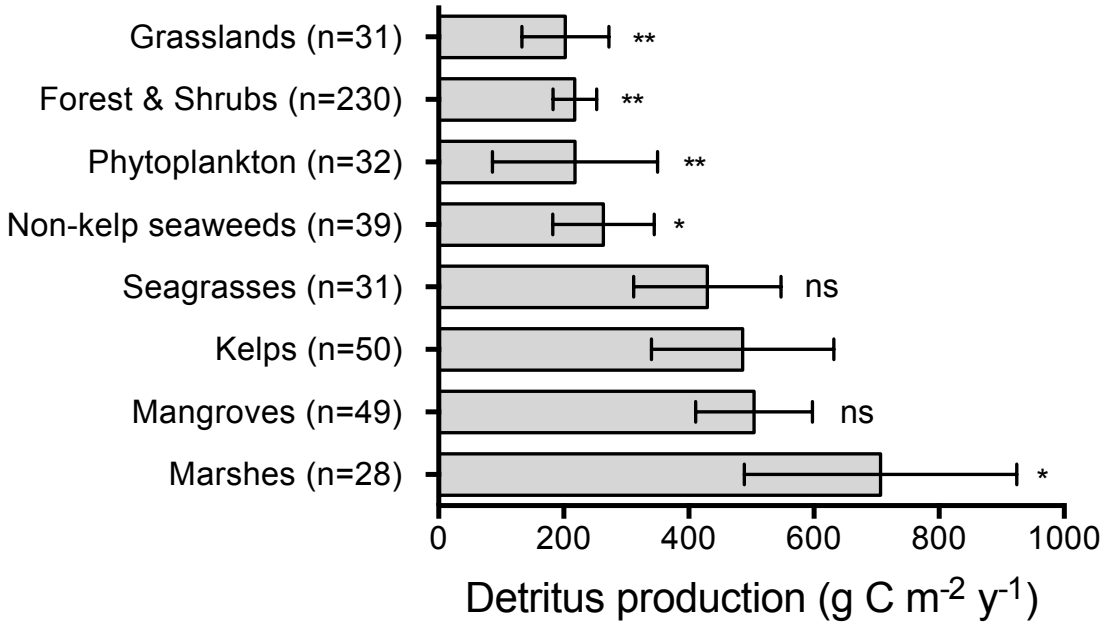

742